Dyadic Wavelet-Based Image Noise Suppression and Enhancement in High-Speed Cardiac MR Parallel Acquisition

Q. Duan[1], J. Chen[1], A. F. Laine[1], and V. M. Pai[2]
[1]Biomedical Engineering, Columbia University, New York, NY, United States, [2]Radiology, SUNY Upstate Medical University, Syracuse, NY, United States

Introduction

Parallel imaging techniques have become important tools in improving acquisition speeds for cardiac MRI data. However, parallel acquisitions involve well-known tradeoffs between acceleration and signal-to-noise ratio (SNR) in the reconstructed images due to the physics of acquisition. For a given field-of-view, increasing the parallel imaging rate in general will lead to a corresponding deterioration in signal quality; the faster the acquisition is, the poorer are the resultant images. Image denoising techniques when used as a post-processing step to a parallel-imaging acquisition may provide a means to push the existing limits of temporal resolution of the cardiac cycle while maintaining image quality for high-speed acquisition protocols. Previously, we have developed a wavelet-based denoising technique [1] in improving the SNR of cardiac imaging during such fast acquisition. In this work, the method was extended to combining image denoising and image enhancement.

Method

The proposed method was based on overcomplete 3D dyadic wavelet expansions. A 3D discrete dyadic wavelet transform of *M* level analysis can be represented as a set of wavelet coefficients: $\left\{S_M s(n_1,n_2,n_3),\left\{W_M^1 s(n_1,n_2,n_3),W_M^2 s(n_1,n_2,n_3),W_M^3 s(n_1,n_2,n_3)\right\}\right\}$, where $W_M^1 s(n_1,n_2,n_3) = < s,\psi^k_{m,n_1,n_2,n_3} >, k=1,2,3$ and $m=1,\cdots,M$. The wavelet bases were dilated and translated from wavelet functions: $\psi^k_{m,n_1,n_2,n_3}(x,y,z)=\frac{1}{2^{3m/2}}\psi^k\left(\frac{x-n_1}{2^m},\frac{y-n_2}{2^m},\frac{z-n_3}{2^m}\right), k=1,2,3$. The processed image $\left|\mathbf{X}_{new}\right\rangle$ was derived by $\left|\mathbf{X}_{new}\right\rangle=\sum_{m=0}^{N-1}\rho_m\left(\left\langle\mathbf{X},\psi_m\right\rangle\right)\psi_m$, where $\mathbf{X}$ was the original image acquired by parallel acquisition, and ρ_m was an adaptive mapping function. By properly choosing ρ_m, noise components can be attenuated or decreasing some coefficient sets in the transform domain while the true signal coefficients can be preserved or enhanced. In our previous application, a soft-thresholding scheme as shown in Fig.1a was applied to suppress the noise component. In this work, to add signal enhancement feature in addition to the denoising feature, a piecewise linear ρ_m as shown in Fig. 1b was adopted. By tuning the turning points and slopes of different segments of ρ_m, image denoising and image enhancement can be seamlessly integrated into one step without any additional computational cost. The algorithm was preliminarily implemented in Matlab© (Natick, MA). For phantom studies, the ACR MR phantom was imaged using a Siemens Avanto 1.5T MR scanner. Both *k*-space-based (using generalized auto-calibrating partially parallel acquisitions; GRAPPA [3]) and image-domain based (using sensitivity encoding, mSENSE [4]) parallel-imaging approaches were used with different parallel imaging rates (or acceleration factors, R). A balanced-SSFP image without parallel acquisition was also acquired as the "best available quality" image. For GRAPPA and mSENSE, protocols with R=2,3 and 4 with 36 reference lines were acquired with additional images at different noise level. Image Contrast-to-Noise Ratio (CNR) for each image was computed using the method described in [2] (CNR=(mean(ROI)-mean(Background))/std(ROI) for homogeneous ROI) within the first three columns of tubes. To explore the feasibility of our denoising approach on clinical data, a healthy volunteer was scanned using a Siemens 1.5T scanner. Cardiac cine images using GRAPPA and mSENSE with R = 2, 3 and 4 with 36 reference lines were acquired. Image SNR for each image was computed within manually picked regions of interest (ROI) within the blood pool in the left ventricle. CNR between the blood pool and the myocardium was computed.

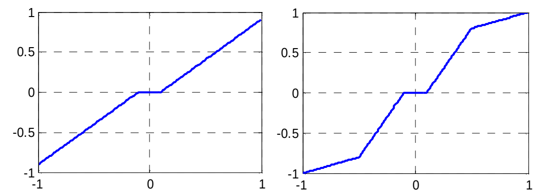

Figure 1: Illustration of transform function: soft thresholding (left) and piecewise linear function (right). X-axis is the original wavelet coefficient and Y-axis is the output wavelet coefficient after denosing/enhancing.

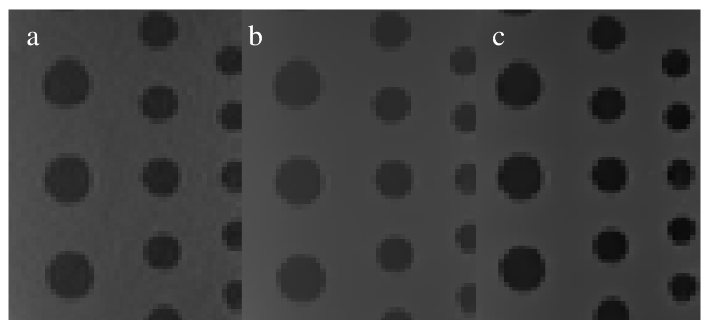

Figure 2: Zoomed ACR Phantom images: (a) Original image acquired by GRAPPA (R=4) (b) filtering result by soft thresholding and (c) filtering result by piecewise linear function.

Results

Fig. 2 shows a zoomed view of an ACR phantom acquired by GRAPPA (R=4) (Fig.2a) and corresponding filtering results by soft-thresholding (Fig.2b) and piecewise linear function (Fig. 2c). Both filtered versions had less noise and the results from the proposed method had better contrast. As shown in Fig.3, on all parallel acquired data, the ratios of CNR gain of the new method to the soft-thresholding are larger than 1. However, this benefit slightly decreased as the R increased. On all 35 clinical data sets, the new method on average has 1.2 times larger gain in CNR than the original soft-thresholding method. Sample results on clinical data are shown in Fig. 4.

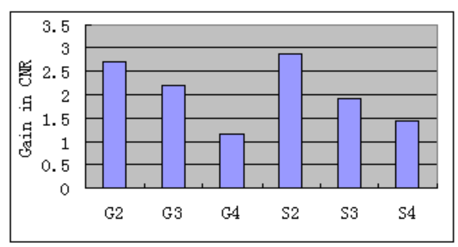

Figure 3: Ratio of CNR gain of the proposed method to soft-thresholding. G:GRAPPA, S:SENSE

Conclusions

An automated integrated denoising/enhancing approach was applied to images acquired by parallel acquisition techniques in cardiac imaging. In comparison with previous denoising only framework, this new proposed method could future increase the CNR of the denoised images. Quantitative evaluation on phantom and clinical data confirmed the benefit of this new method in terms of improving CNR on parallel MR images. Preliminary results suggested that this new integrated denoising/enhancing framework could further push the limits on the temporal resolution by improving the SNR and CNR simultaneously.

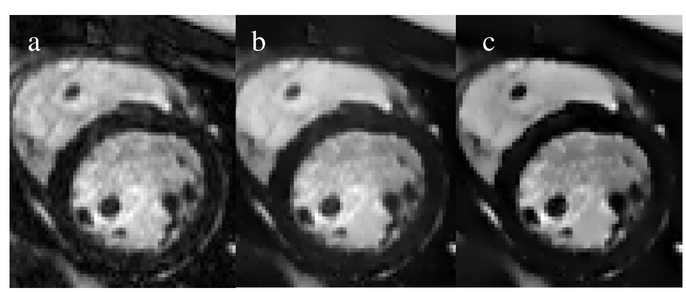

Figure 4: Zoomed cardiac images: (a) Original image acquired by SENSE (R=3) (b) filtering result by soft thresholding and (c) filtering result by piecewise linear function.

References

[1] Q. Duan, et al, ISMRM 2007. [2] V. S. Lee, Lippincott Williams & Wilkins, 2006. [3] Griswold MA,et al, Magn Reson Med 2002;47(6):1202-1210. [4] Pruessmann KP, et al, Magn Reson Med 1999;42(5):952-962.